A Deep Support Vector Data Description Method for Anomaly Detection in Helicopters

Chenyu Liu[1,2] and Konstantinos Gryllias[1,2]

[1] *Division Mecha(tro)nic System Dynamics, Department of Mechanical Engineering, KU Leuven*
[2] *Dynamics of Mechanical and Mechatronic Systems, Flanders Make*
Celestijnenlaan 300, BOX 2420, 3001 Leuven, Belgium
chenyu.liu@kuleuven.be, konstantinos.gryllias@kuleuven.be

Abstract

Helicopters are high-value mechanical assets which have gained much attention from condition monitoring practitioners. Modern helicopter health management system leverages various sensors to collect in-flight signals. In order to trigger an alarm when an anomaly happens, signal processing methods are used to construct health indicators that require expert knowledge. On the other hand, classic features are always case-specific and may fail to discriminate anomalies in practical applications. Support Vector Data Description (SVDD) is a machine learning method used as a one-class classifier to serve anomaly detection tasks. It utilizes healthy samples to construct a hypersphere feature space as a detection threshold. In order to automate the anomaly detection pipeline, a deep SVDD model is proposed in this paper. A Convolutional Neural Network (CNN) is used as the feature extractor, which provides smart features to an SVDD model. The SVDD model uses a soft-boundary hyper-sphere for decision-making. The optimization of the CNN and the SVDD is connected, which makes it an end-to-end process. The methodology is applied, tested and evaluated on a helicopter vibration dataset, which has been provided by Airbus SAS in the frames of an AI Gym challenge. The experimental results reveal that the F_1 score of the proposed Deep SVDD can reach 94%, showing its compelling efficacy for anomaly detection.

1. Introduction

Modern sensor technologies give access to ever-increasing amounts of data captured from mechanical assets, enabling the evolving of condition monitoring from after-the-fact maintaining into real-time assessment. Since the time maintenance engineers were able to digitally collect online measurements, anomaly detection has become one of the main elements in advanced condition monitoring for early warning of machinery's degradation. In the aviation industry, an accuracy-assured anomaly detection system is of utmost importance for the aircraft's proactive maintaining operations.

Helicopters are high-value assets which have gained much attention from condition monitoring practitioners (Samuel & Pines, 2005). Vibration sensors have been widely integrated into helicopters as the primary surveillance tool due to the convenient acquisition and the contained abundant signature information (Schmidt et al., 2020). Classic vibration-based anomaly detection relies on hand-crafted health indicators, also known as feature engineering. Signal processing approaches, such as spectrum analysis (Jin et al., 2016), time-frequency analysis (Purushotham et al., 2005), cyclic spectral analysis (Randall et al., 2001; Antoni, 2009; Mauricio et al., 2020), and empirical mode decomposition (Dybała & Zimroz, 2014), have been vastly used for the feature engineering process. These methods require expert knowledge to manually construct features in order to reflect the health conditions. On the other hand, classic features are always case-specific and may fail to accurately discriminate the anomalies in practical applications, especially for incipient or compound defects (Chen et al., 2019).

In the last years, Machine Learning (ML) is quickly sweeping into every corner of both academia and industry, transforming the condition monitoring community. Various ML models have been developed and proved efficient to facilitate the anomaly detection process. Combined with classic feature engineering, ML can be used to dig the discriminative information between normal and abnormal data. Yiakopoulos et al. (2011) developed a K-means clustering method with time and frequency domain features for unsupervised bearing fault detection. Support Vector Machine (SVM) is a kernel-based machine learning method that has been widely used. Gryllias and Antoniadis (2012) applied an SVM trained by features from simulation data on a real dataset to detect bearing defects. Saari et al. (2019) utilized an SVM to detect windmill bearing faults with frequency domain features as inputs.

Support Vector Data Description (SVDD) is another kernel-based machine learning method used as a one-class classifier to serve anomaly detection tasks (Tax & Duin, 1999, 2004). It utilizes healthy samples to construct a hyper-sphere feature space as the detection threshold. SVDD method has delivered some heuristic findings in condition monitoring research. Liu and Gryllias (2020) constructed frequency domain features using cyclic spectral analysis and used them within the SVDD frame. This method has been proved robust against outliers and can achieve a high detection rate for bearing anomaly detection. However, the inherent limitation of SVDD is still distinct in terms of application: hand-craft indicators are inevitable as intermediaries between the raw input signals and the SVDD model.

With the development of artificial intelligence, ML is now upgrading toward an end-to-end solution. Deep neural network, or deep learning method, came into large-scale application in 2010 and now becomes a significant branch of ML. A deep neural network consists of multiple hidden layers and is able to decompose the inputs into intrinsic characteristics, therefore can better perceive the hierarchical information (Goodfellow et al., 2016). Deep learning method is able to extract smart features from the raw inputs instead of feature engineering, thus provides an extremely effective approach to process a large amount of data.

Anomaly detection tasks have been extensively studied using deep neural networks, and most of these methods are based on input reconstruction. For instance, Zhang et al. (2019) trained a Variational Autoencoder (VAE) with healthy bearing signals. The VAE is expected to learn the pattern of healthy operating conditions during reconstruction. Once a high residual between the measurement and the reconstruction is observed, it is considered an anomaly. A similar reconstruction can also be found using Long Short-Term Memory (LSTM) network (Malhotra et al., 2016), Convolutional Autoencoder (CAE) (Garcia et al., 2020) or Generative Adversarial Network (GAN) (Jiang et al., 2019).

Combining neural networks with SVDD can exploit both the smart features and the robust detector. Deep SVDD was proposed by Ruff et al. (2018) as an automated anomaly detection method that is able to conjunct any network with the SVDD model. The synchronized optimization can make the smart features compact around the center of the sphere, thus can separate the anomaly data points.

In this paper, a Convolutional Neural Network (CNN)-based deep SVDD model is proposed for helicopter anomaly detection. The raw vibration signals are sent to a deep CNN for feature extraction. The smart features are then fed to an SVDD model to construct the hyper-sphere for decision-making. The optimization of the CNN and the SVDD is connected, which makes it an end-to-end process. The methodology is applied, tested and evaluated on a helicopter vibration dataset, which has been provided by Airbus SAS in the frames of an AI Gym challenge.

The rest of the paper is organized as follows: Section II introduces the theoretical background of kernel-based SVDD and deep SVDD. The proposed CNN-based deep SVDD architecture is discussed in Section III. The experimental dataset, the evaluation metrics, and comparative methods are presented in Section IV. Section V discusses the experimental results. The paper ends with some conclusions in the last section.

2. Theory of Support Vector Data Description

2.1. Kernel-based SVDD classifier

Support Vector Data Description is a kernel-based classification method and was initially proposed as an unsupervised one-class classifier (Tax & Duin, 1999). Inspired by the classic One-Class Support Vector Machine (OC-SVM), SVDD uses a hyper-sphere instead of a hyper-plane to separate the normal data from the anomalous. The sketch of SVDD characterized by center a and radius R is shown in Figure 1.

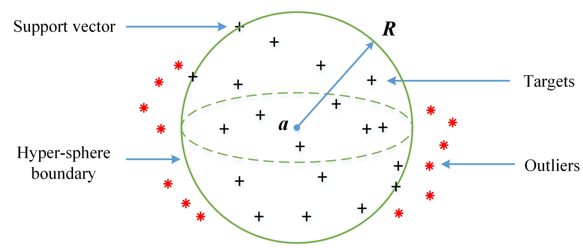

Figure 1. The sketch of SVDD.

Consider $\mathcal{X} \subseteq \mathbb{R}$ is the input data space and $\phi_k(x_i) : \mathcal{X} \rightarrow \mathcal{H}_k$ is the mapping function with kernel $k : \mathcal{X} \times \mathcal{X} \rightarrow [0, +\infty)$. $\mathcal{H}_k$ is the dot product space, which is also known as the feature space. When an input dataset is given as $\mathcal{D} = \{x_1, \cdots, x_n\}$ with $x_i \in \mathcal{X}$, SVDD will try to find a hyper-sphere containing the majority of the data objects in $\mathcal{H}_k$ with the minimum volume. The primal problem of SVDD can be described as:

$$\begin{aligned} \min \; & R^2 + \frac{1}{\nu n} \sum_{i=1}^{n} \xi_i \\ s.t. \quad & \|\phi_k(x_i) - a\|^2 \leq R^2 + \xi_i \quad \forall i, \xi_i \geq 0 \end{aligned} \tag{1}$$

where R and a are the radius and the center of the sphere, respectively. ξ_i is the slack variable which allows some of the samples exist outside the sphere boundary. $\nu \in (0, 1]$ is the penalty parameter controlling the trade-off between the sphere volume and the number of rejected data samples, which provides an efficient way to measure the fraction of training data outliers.

It should be noticed that Eq. 1 cannot be solved for an unknown R since it is a convex quadratic programming problem. It needs to be transformed to the respective dual problem via

Lagrange duality (Tax & Duin, 1999). Then the constraint conditions can be integrated into Eq. 1, which can be described with the dual form as follows:

$$L = \max \sum_{i=1}^{n} \alpha_i (x_i \cdot x_i) - \sum_{i,j} \alpha_i \alpha_j (x_i \cdot x_j) \tag{2}$$

where $(x_j \cdot x_i)$ denotes the inner product and $\alpha_i \in \mathbb{R}$ are the Lagrange multipliers. Eq. 2 can be solved when introducing a kernel function inside, as illustrated by Tax and Duin (2004).

SVDD has been proved effective in many applications, but there are still two drawbacks to the method. Firstly, it requires explicit feature engineering as the prior step, and low-quality features might jeopardize the classification task. Secondly, the kernel matrix restricts its computational efficiency and needs more memory to store the support vectors in practical usage (Ruff et al., 2018).

2.2. Theory of Deep SVDD

Deep neural network provides a novel approach to get the discriminative features from the raw data. The features extracted from a deep neural network can be defined as $\phi(\cdot;\mathcal{W}) : \mathcal{X} \to \mathcal{H}$ with the network weights $\mathcal{W} = \{\mathbf{W}^1, \cdots, \mathbf{W}^L\}$, where $\mathbf{W}^l$ represents the weight of hidden layer l. In order to learn the network parameter $\mathcal{W}$ simultaneously minimizing the SVDD hyper-sphere volume, the objective function of one-class deep SVDD can be defined as (Ruff et al., 2018):

$$\min \frac{1}{n} \sum_{i=1}^{n} \|\phi(x_i;\mathcal{W}) - a\|^2 + \frac{\lambda}{2} \sum_{l=1}^{L} \|\mathcal{W}^l\|_F{}^2 \tag{3}$$

where a denotes the center of the sphere, and $\|\cdot\|_F$ is the Frobenius norm. The first term of Eq. 3 simply computes the quadratic loss based on the distances to the sphere center. The second term represents a weight decay regularizer of $\mathcal{W}$ with $\lambda > 0$ introduced as a hyperparameter.

Eq. 3 indicates that the characterizing of the sphere in one-class deep SVDD only needs the center a, while the contraction of the sphere is achieved by the mean value of the distances from every feature to a. One-class deep SVDD strictly encloses every sample from the training set into the sphere, which does not have a tolerance to the outliers. A more flexible form of deep SVDD with soft boundary is also proposed as follows:

$$\begin{aligned} &\min R^2 + \frac{1}{\nu n} \sum_{i=1}^{n} \max \{0, \|\phi(x_i;\mathcal{W}) - a\|^2 - R^2\} \\ &+ \frac{\lambda}{2} \sum_{l=1}^{L} \|\mathcal{W}^l\|_F{}^2 \end{aligned} \tag{4}$$

Comparing to the previous form, soft-boundary deep SVDD characterize the sphere with both the center a and the radius R. A penalty is introduced as the second term in Eq. 4, where $\nu \in (0, 1]$ controls the trade-off with the same function as in Eq. 1.

To achieve the optimization goal, the deep SVDD model must extract the features from the data and map them as close as possible to the center. During the anomaly detection process, data from the normal class will stay compact in the sphere, while the anomalous data points will be mapped on the contrary, far from the center.

3. Proposed Method

Based on the deep SVDD theory, a CNN-based SVDD model is proposed in this paper. The 1D time sequence is used as inputs of the model. The feature extractor consists of four 1D CNN modules with ReLU activations and Batch Normalization (BN) layers. The last CNN module contains a 1D Adaptive Maxpooling (AdpMP1d) layer in order to reduce the dimension of the features space. After the flatten layer, the features are sent through two Fully Connected (FC) layers and then mapped to the Hilbert space with the SVDD. Detailed hyper-parameters of these layers can be found in Figure 2.

The training algorithm of the proposed method is described in Algorithm 1. The soft-boundary deep SVDD is connected to the network outputs in the proposed architecture with center a and radius R. The initialization of a and R follows the work of Ruff et al. (2018) where a is the mean value from an initial forward pass of the training samples, and R is initialized from 0. The hyper-parameter ν is set to 0.1, which provides a flexible boundary to reduce the influence from outliers.

Algorithm 1: CNN-based Deep SVDD for unsupervised anomaly detection

Input: Training dataset $\mathcal{D}_{train} = \{x_1, \cdots, x_n\}$

```
Initialize the weights of CNN and a and R of the SVDD;
for each training iteration step do
    Sample minibatch from the training data D_train;
    Forward propagation through the CNN and the SVDD;
    Calculate the loss based on Eq. (4) ;
    Backpropagate of the gradient using the Adam optimizer for
      the features φ(x_i; W) downsteam the network;
    Update the network weights W and radius R based on
      mini-batch distances;
end
Evaluate the model with testing data D_test
```

During the model training process, some other hyper-parameters are set as follows: the learning rate is set to 10^{-4}; the training epochs are set to 50; a weight decay with 10^{-6} is set for the deep SVDD objective.

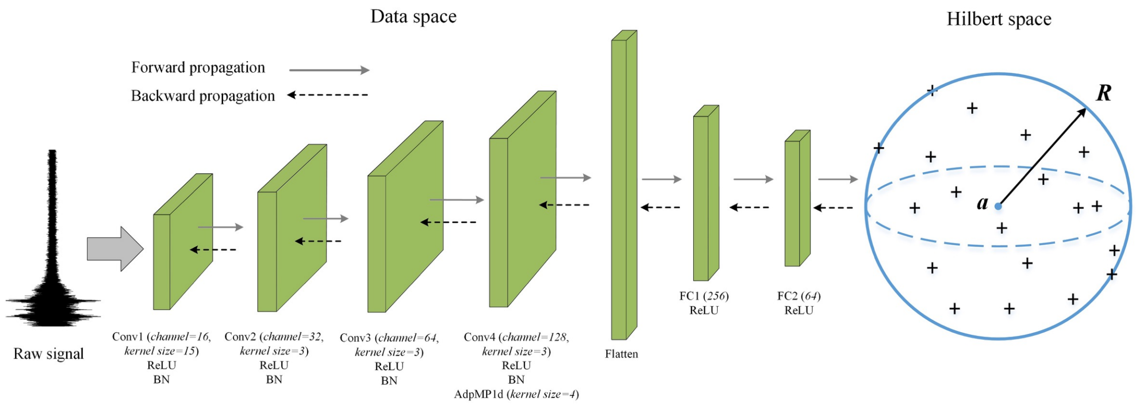

Figure 2. The architecture of CNN-based deep SVDD for anomaly detection.

The entire pipeline of implementing the proposed method can be found in Figure 3. Signals from the healthy operating condition, which usually exist at the beginning of the experiment, are used to train the deep SVDD model. Then the incoming signals are tested by the model for anomaly detection.

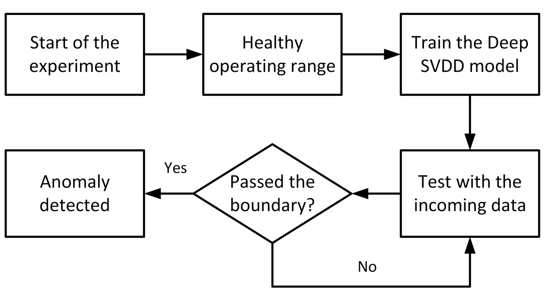

Figure 3. Time domain features of the training dataset.

4. Experiments

4.1. Experimental dataset

Airbus SAS released an experimental dataset during an AI Gym anomaly detection challenge, which contains vibration signals measured from accelerometers mounted on different positions and axes on Airbus helicopters (Garcia et al., 2020). The sampling frequency of the signals is 1024 Hz. The dataset consists of a training set with 1677 sequences collected from normal flights and a validation set with 594 sequences from normal and abnormal flights. Each sequence represents a continuous time series of 60s with a length of 61440 points.

The primary task of the challenge was to train a detector with only healthy data in the training set and test the detection performance with a validation set without prior knowledge about the anomalies. This fits well with the practical anomaly detection scenarios where the maintenance engineer is capturing most of the time healthy data.

4.2. Evaluation metrics

The confusion matrix of a binary classifier can be found in Figure 4. Based on the estimated label and the corresponding true label, the classification results could fall into four areas, i.e., True Negative (TN), False Negative (FN), False Positive (FP), and True Positive (TP).

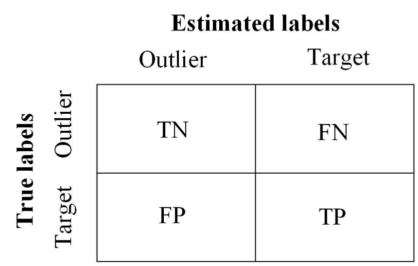

Figure 4. Calculation of the evaluation metrics.

Three evaluation metrics can be calculated based on the confusion matrix, including the True Positive Rate (TPR), the False Positive Rate (FPR), and the F_1 score, as illustrated below:

$$TPR = \frac{TP}{FN + TP} \tag{5}$$

$$FPR = \frac{FP}{TN + FP} \tag{6}$$

$$F_1 = \frac{2 \cdot TP}{2 \cdot TP + FP + FN} \tag{7}$$

TPR represents the proportion of true positive predictions, which is also called Recall. FPR computes the false positive predictions over all the ground truth negatives. F_1 is the harmonic average of Recall and Precision, which is the positive prediction value.

Besides the three metrics derived from the confusion matrix, the Receiving Operator Curve (ROC) and the Area Under

Curve (AUC) are also used to measure the detection efficacy. Besides, the model training time is also recorded for the deep learning models to compare the computational efficiency.

4.3. Comparative methods

4.3.1. Baseline SVDD model with engineered features

The classic one-class SVDD model with engineered features is adopted as the baseline model. As listed in Table 1, nine time-domain health indicators are computed for each sample, forming an input matrix with shape (61440, 9). The hyper-parameter ν of the SVDD is set to 0.1.

4.3.2. Deep SVDD with different feature extractors

The comparative analysis is carried among different input types. Instead of using the raw time sequence, the FFT spectrum with size (30700,1) is used as the 1D inputs for the proposed CNN-based SVDD model. Further, a Bi-directional Long Short-Term Memory (Bi-LSTM) network is also used as the feature extractor combining the SVDD model with both the time series and the FFT spectrum as inputs. The architecture and the hyper-parameters setting of the Bi-LSTM follow the work of Zhou et al. (2016).

2D inputs are also examined in the deep SVDD frame. The time series is transformed into 2D representations with three methods:

- *2D Slices*: The raw time sequence is reshaped into a 2D matrix with a size (60, 1024) along the second dimension. Therefore, each row represents a slice of the time signal of 1 second.
- *2D STFT spectrogram*: Short Time Fourier Transform (STFT) is adopted on the raw signal. A Hann window is used with a size of 256 points and an overlap of 128 points. The input shape is (128, 481).
- *2D WPD spectrogram*: Wavelet Packet Decomposition (WPD) is applied in the level of 8. The input shape of the 2D WPD spectrogram is (256, 61440).

Consequently, two classic 2D deep models are adopted to fit these inputs, including a LeNet 2D model and a ResNet 2D model. The hyper-parameters settings of LeNet follows the work of LeCun et al. (1998), and the ResNet follows the work of He et al. (2016)

4.3.3. Reconstruction-based deep models

Reconstruction-based methods are considered as strong competitors since they have been proved efficient in different anomaly detection cases. The candidates are selected, including an LSTM model, a VAE model and a GAN model. The LSTM model utilizes the architecture proposed by Malhotra et al. (2016). The VAE and the GAN model follows the parameter settings in the paper by Zhang et al. (2019) and Jiang et al. (2019), respectively. Garcia et al. (2020) applied CAE on this dataset; therefore, the results from the CAE model with spectrogram inputs will be introduced for comparison. Besides the model architecture and hyper-parameters, one of the critical issues for these methods is the decision-making process dealing with the reconstruction error. For simplicity, a statistic-based thresholding process used by Garcia et al. (2020) is also applied.

5. Results

The proposed model is achieved with Python 3.6 and PyTorch 1.1.0. The computational experiments are conducted on an Intel Xeon Gold 6140 (2.3 GHz) with NVIDIA Tesla P100 GPU acceleration.

5.1. Complexity analysis of the proposed model

The computational time complexity of the proposed CNN-based deep SVDD model is analyzed based on the time cost of the convolutional layers described as follows (He & Sun, 2015):

$$O(\sum_{l=1}^{d} n_{l-1} \cdot s_l^2 \cdot n_l \cdot m_l^2) \tag{8}$$

where l represents the convolutional layer index. For the l-th convolutional layer, n_{l-1} is the number of the input channels. s_l is the length of the filter and m_l is the size of the feature map. In the proposed CNN-based deep SVDD model, the depth of the convolutional layer d=4, therefore the theoretical time complexity of the CNN part can be calculated following Eq. 8. It should be noticed that the complexity value is different from actual model training time depending on the computational resource. Besides the convolutional layer, the pooling layer and the fully connected layer take 5-10% of the computational time. For comparative analysis of different CNN structures within the proposed method, the complexity values are discussed in Section 5.3.

5.2. Comparative analysis against the baseline model

As discussed in the previous section, the baseline SVDD model requires time domain features to construct the input data space. The features of the training samples are plotted in the waterfall as shown in Figure 5. It can be seen that, although all the samples come from the normal condition, some of these features fluctuate in a wide range, such as STD, CF, IF, and CLF, indicating these features are not robust enough to reflect the health conditions of the helicopter.

The anomaly detection results are shown in Table 2, where the proposed method outperforms the baseline model in all the metrics. For the critical F_1 score, deep SVDD yields a 0.14 boost.

On the one hand, the results indicate that the selected time-

Table 1. Features from the time domain.

RMS	$RMS = \sqrt{\frac{\frac{1}{n}\sum_{i=1}^{n} x_i^2}{n}}$	Variance	$VR = \frac{\sum_{i=1}^{n}(x_i-m)^2}{(n-1)\sigma^2}$	Shape Factor	$SF = \frac{\sqrt{\frac{1}{n}\sum_{i=1}^{n} {x_i}^2}}{\frac{1}{n}\sum_{i=1}^{n}\|x_i\|}$
Kurtosis	$KU = \frac{\sum_{i=1}^{n}(x_i-m)^4}{(n-1)\sigma^4}$	Mean	$m = \frac{\sum_{i=1}^{n} x_i}{n}$	Impulse Factor	$IF = \frac{\max\|x_i\|}{\frac{1}{n}\sum_{i=1}^{n}\|x_i\|}$
Skewness	$SK = \frac{\sum_{i=1}^{n}(x_i-m)^3}{(n-1)\sigma^3}$	Crest Factor	$CF = \frac{\max\|x_i\|}{\sqrt{\frac{1}{n}\sum_{i=1}^{n} {x_i}^2}}$	Clearance Factor	$CLF = \frac{\max\|x_i\|}{(\frac{1}{n}\sum_{i=1}^{n}\sqrt{\|x_i\|})^2}$

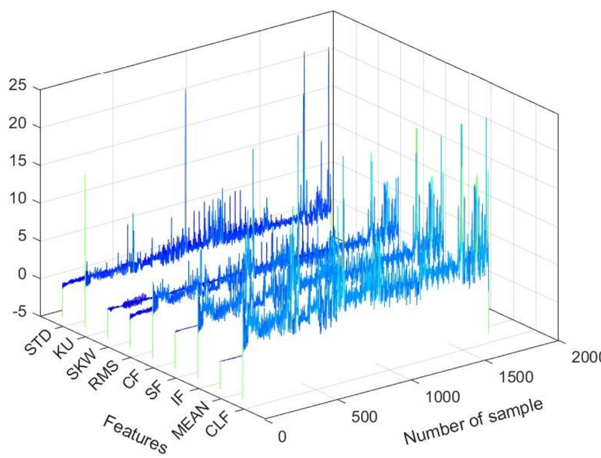

Figure 5. Time domain features of the training dataset.

Table 2. Anomaly detection results of the baseline and the proposed models.

	TPR	FPR	F_1	AUC
Baseline model	0.86	0.29	0.80	0.76
Proposed model	**0.91**	**0.02**	**0.94**	**0.94**

domain features fail to capture the health-related information from the raw vibration signals. On the other hand, the CNN layers of the deep SVDD can extract discriminative representations from the time series while building a robust SVDD boundary to isolate the anomalous samples. The ROC curve and the corresponding AUC value of the two models can be found in Figure 6a.

5.3. Comparative analysis of the feature extractors

Experimental results of the 1D input deep SVDD models are shown in Table 3. For the two input types, the 1D time series outperforms the 1D FFT spectrum in both models except the training time due to the FFT spectrum is half the length of the raw time sequence. The complexity values of CNN-based feature extractors are calculated relative to the 1D time series input. The results of the CNN-based model show significant leads in almost all the metrics. Compared to the 1D-LSTM network, the F_1 score of 1D-CNN with time series yields a significant 0.32 boost, and the lead extends to 0.38 for 1D FFT spectrum inputs.

It is noticeable that the lowest FPR=0 is observed in 1D-LSTM with FFT. This indicates that the model does not mislabel normal samples as abnormal. Considering the low TPR of this model, there is a strong possibility that the SVDD has a high boundary with a high acceptance rate for normal samples. The ROC curve of the 1D-CNN and 1D-LSTM SVDD models can be found in Figure 6b and 6c, respectively.

The results of the 2D input models are presented in Table 4. Generally, the 2D-LeNet with the STFT spectrogram outperforms the others. In the 2D-LeNet model, both the F_1 scores and the AUC of the STFT and WPD are very close. However, the model complexity value and the training time of WPD is over three times the STFT due to the large matrix size. The detection performance of the 2D-LeNet and 2D-ResNet models are similar for STFT and WPD inputs, but the performance of ResNet decreased over 0.2 when using 2D slices input. The ROC curves of the 2D models are presented in Figure 6b and 6c.

In general, the 1D-CNN model with the time series as inputs reach the top performance but are sensitive to the feature extractor. The changing of the network influences more its detection performance. On the other hand, the STFT and WPD inputs are more robust to different networks. It is possible that more discriminate features are exposed after the STFT and the WPD process, which makes them robust to different network architectures.

5.4. Results from reconstruction-based models

Table 5 shows the detection results of the reconstruction-based deep models. The ROC curves of LSTM, VAE and GAN are shown in Figure 6f. In general, the reconstruction-based methods show relatively high detection accuracy preliminary due to the strong feature extraction ability of the deep networks. 2D-CAE gives the best results among the four methods with slightly higher F_1 and AUC value. The most distinct advantage of CAE is its low computation cost, which needs less than half of the others' model training time.

The proposed method outperforms the reconstruction-based models, which yields an improvement of 0.02 comparing to the best of these three methods, but takes relatively longer

Table 3. Results of the deep SVDD models with 1D feature extractors.

Input type	1D-CNN						1D-LSTM					
	TPR	FPR	F1	AUC	Comp.	Time (s)	TPR	FPR	F1	AUC	Comp.	Time (s)
1D Time series	**0.91**	0.02	**0.94**	**0.94**	1.00	184	0.49	0.09	0.62	0.70	1.21	203
1D FFT spectrum	0.89	0.19	0.86	0.85	**0.54**	**96**	0.31	**0.00**	0.48	0.66	0.59	104

Table 4. Results of the deep SVDD models with 2D feature extractors.

Input type	LeNet 2D						ResNet 2D					
	TPR	FPR	F1	AUC	Comp.	Time (s)	TPR	FPR	F1	AUC	Comp.	Time (s)
2D Slices	0.82	0.20	0.81	0.81	2.40	424	0.35	**0.00**	0.52	0.59	2.38	416
2D STFT spectrogram	0.90	**0.04**	**0.92**	**0.93**	2.10	360	0.85	0.09	0.87	0.89	**1.82**	**325**
2D WPD spectrogram	**0.91**	0.08	0.91	0.91	6.65	1223	0.89	0.08	0.90	0.90	5.80	1054

model training time. Reducing the hyper-parameter number meanwhile keeping the high performance for Deep SVDD could be the direction for the following research work.

6. Conclusion

A CNN-based deep SVDD model is proposed for helicopter anomaly detection in this paper. The proposed method uses raw vibration signals as inputs, which are further sent to a deep CNN for feature extraction. The smart features are mapped to an SVDD model in order to construct a hyper-sphere fea-

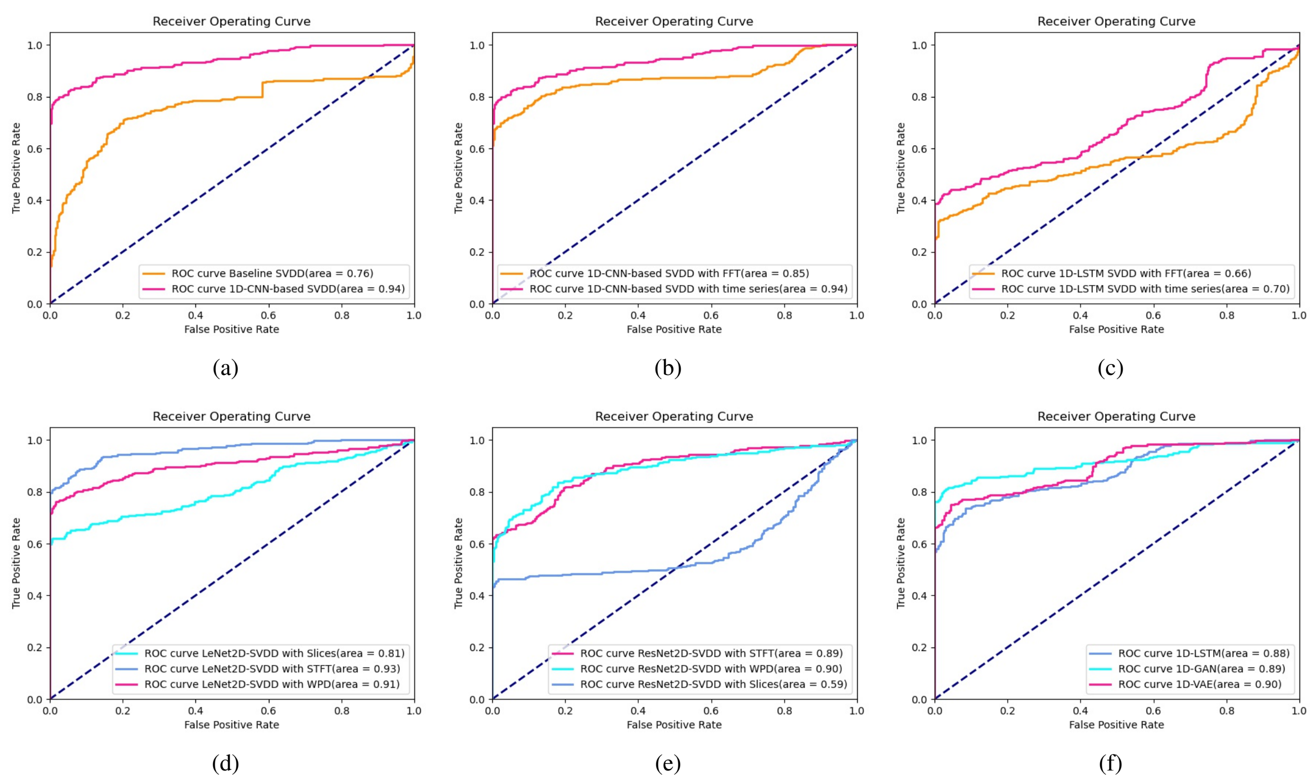

Figure 6. ROC curves from different anomaly detection models. (a) Baseline and the proposed model. (b) 1D-CNN-based deep SVDD. (c) 1D-LSTM-based deep SVDD. (d) 2D-LeNet-based deep SVDD. (e) 2D-ResNet-based deep SVDD. (f) Reconstruction-based deep models.

Table 5. Anomaly detection results of reconstruction-based deep models.

	TPR	FPR	F_1	AUC	Time (s)
1D-LSTM	0.82	0.12	0.87	0.88	162
1D-VAE	0.88	0.08	0.90	0.90	135
1D-GAN	0.84	0.09	0.86	0.89	326
2D-CAE Garcia et al. (2020)	0.85	**0.01**	0.91	0.92	**62**

ture space. The optimization of the CNN and the SVDD is connected which makes it an end-to-end model. Experiments are carried based on a helicopter vibration dataset provided by Airbus SAS, and the method is proved efficient to deal with the anomaly detection task. Comparative analysis shows that the proposed method with 1D time series input obtains better performance than the 1D FFT spectrum, 2D time series slices, 2D STFT spectrogram and 2D WT spectrogram inputs. Meanwhile, the CNN-based deep SVDD model achieves higher detection accuracy than state-of-the-art reconstruction-based deep learning detection models.

ACKNOWLEDGMENT

The authors would like to acknowledge the support of the China Scholarship Council, the Flemish Government under the "Onderzoeksprogramma Artificiële Intelligentie (AI) Vlaanderen" programme, Flanders Make the strategic research centre for the manufacturing industry in the context of DGTwin Prediction project, the Flemish Supercomputer Center (VSC) for the computation resource.

REFERENCES

Antoni, J. (2009). Cyclostationarity by examples. *Mechanical Systems and Signal Processing*, *23*(4), 987–1036.

Chen, Z., Gryllias, K., & Li, W. (2019). Intelligent fault diagnosis for rotary machinery using transferable convolutional neural network. *IEEE Transactions on Industrial Informatics*, *16*(1), 339–349.

Dybała, J., & Zimroz, R. (2014). Rolling bearing diagnosing method based on empirical mode decomposition of machine vibration signal. *Applied Acoustics*, *77*, 195–203.

Garcia, G. R., Michau, G., Ducoffe, M., Gupta, J. S., & Fink, O. (2020). Time series to images: Monitoring the condition of industrial assets with deep learning image processing algorithms. *arXiv preprint arXiv:2005.07031*.

Goodfellow, I., Bengio, Y., Courville, A., & Bengio, Y. (2016). *Deep learning* (Vol. 1) (No. 2). MIT press Cambridge.

Gryllias, K. C., & Antoniadis, I. A. (2012). A support vector machine approach based on physical model training for rolling element bearing fault detection in industrial environments. *Engineering Applications of Artificial Intelligence*, *25*(2), 326–344.

He, K., & Sun, J. (2015). Convolutional neural networks at constrained time cost. In *Proceedings of the ieee conference on computer vision and pattern recognition* (pp. 5353–5360).

He, K., Zhang, X., Ren, S., & Sun, J. (2016). Deep residual learning for image recognition. In *Proceedings of the ieee conference on computer vision and pattern recognition* (pp. 770–778).

Jiang, W., Hong, Y., Zhou, B., He, X., & Cheng, C. (2019). A gan-based anomaly detection approach for imbalanced industrial time series. *IEEE Access*, *7*, 143608–143619.

Jin, X., Sun, Y., Que, Z., Wang, Y., & Chow, T. W. (2016). Anomaly detection and fault prognosis for bearings. *IEEE Transactions on Instrumentation and Measurement*, *65*(9), 2046–2054.

LeCun, Y., Bottou, L., Bengio, Y., & Haffner, P. (1998). Gradient-based learning applied to document recognition. *Proceedings of the IEEE*, *86*(11), 2278–2324.

Liu, C., & Gryllias, K. (2020). A semi-supervised support vector data description-based fault detection method for rolling element bearings based on cyclic spectral analysis. *Mechanical Systems and Signal Processing*, *140*, 106682.

Malhotra, P., Ramakrishnan, A., Anand, G., Vig, L., Agarwal, P., & Shroff, G. (2016). Lstm-based encoder-decoder for multi-sensor anomaly detection. *arXiv preprint arXiv:1607.00148*.

Mauricio, A., Smith, W. A., Randall, R. B., Antoni, J., & Gryllias, K. (2020). Improved envelope spectrum via feature optimisation-gram (iesfogram): A novel tool for rolling element bearing diagnostics under non-stationary operating conditions. *Mechanical Systems and Signal Processing*, *144*, 106891.

Purushotham, V., Narayanan, S., & Prasad, S. A. (2005). Multi-fault diagnosis of rolling bearing elements using wavelet analysis and hidden markov model based fault recognition. *Ndt & E International*, *38*(8), 654–664.

Randall, R. B., Antoni, J., & Chobsaard, S. (2001). The relationship between spectral correlation and envelope analysis in the diagnostics of bearing faults and other cyclostationary machine signals. *Mechanical systems and signal processing*, *15*(5), 945–962.

Ruff, L., Vandermeulen, R., Goernitz, N., Deecke, L., Siddiqui, S. A., Binder, A., … Kloft, M. (2018). Deep one-class classification. In *International conference on machine learning* (pp. 4393–4402).

Saari, J., Strömbergsson, D., Lundberg, J., & Thomson, A. (2019). Detection and identification of windmill bearing faults using a one-class support vector machine (svm). *Measurement*, *137*, 287–301.

Samuel, P. D., & Pines, D. J. (2005). A review of vibration-based techniques for helicopter transmission diagnostics. *Journal of sound and vibration*, *282*(1-2), 475–508.

Schmidt, S., Mauricio, A., Heyns, P. S., & Gryllias, K. C. (2020). A methodology for identifying information rich frequency bands for diagnostics of mechanical components-of-interest under time-varying operating conditions. *Mechanical Systems and Signal Processing*, *142*, 106739.

Tax, D. M., & Duin, R. P. (1999). Support vector domain description. *Pattern recognition letters*, *20*(11-13), 1191–1199.

Tax, D. M., & Duin, R. P. (2004). Support vector data description. *Machine learning*, *54*(1), 45–66.

Yiakopoulos, C., Gryllias, K. C., & Antoniadis, I. A. (2011). Rolling element bearing fault detection in industrial environments based on a k-means clustering approach. *Expert Systems with Applications*, *38*(3), 2888–2911.

Zhang, S., Ye, F., Wang, B., & Habetler, T. G. (2019). Semi-supervised learning of bearing anomaly detection via deep variational autoencoders. *arXiv preprint arXiv:1912.01096*.

Zhou, P., Shi, W., Tian, J., Qi, Z., Li, B., Hao, H., & Xu, B. (2016). Attention-based bidirectional long short-term memory networks for relation classification. In *Proceedings of the 54th annual meeting of the association for computational linguistics (volume 2: Short papers)* (pp. 207–212).

BIOGRAPHIES

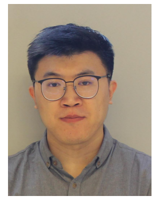

Chenyu Liu received the B.S. and M.Sc degree in aircraft manufacturing engineering and solid mechanics both from Northwestern Polytechnical University, China. He joined the Noise and Vibration Research Group in the Department of Mechanical Engineering, KU Leuven, Belgium as a PhD researcher in 2017. His research interests include data-driven based condition monitoring, rotating machinery prognostics, and machine learning and deep learning application.

Konstantinos Gryllias holds a 5 years engineering diploma degree and a PhD degree in Mechanical Engineering from National Technical University of Athens, Greece. He holds an associate professor position on vibro-acoustics of machines and transportation systems at the Department of Mechanical Engineering of KU Leuven, Belgium. He is also the manager of the University Core Lab Dynamics in Mechanical & Mechatronic Systems DMMS-M of Flanders Make, Belgium. His research interests lie in the fields of condition monitoring, signal processing, prognostics and health management of mech. & mechatronic systems.